



High-efficiency graphene nanomesh magnets realized by controlling monohydrogenation of pore edges

T. Kato, T. Nakamura, J. Kamijyo, T. Kobayashi, Y. Yagi, and J. Haruyama

Citation: [Applied Physics Letters](#) **104**, 252410 (2014); doi: 10.1063/1.4885390

View online: <http://dx.doi.org/10.1063/1.4885390>

View Table of Contents: <http://scitation.aip.org/content/aip/journal/apl/104/25?ver=pdfcov>

Published by the [AIP Publishing](#)

Articles you may be interested in

[Electric field control of spin-resolved edge states in graphene quantum nanorings](#)

J. Appl. Phys. **115**, 174310 (2014); 10.1063/1.4874939

[Magnetic edge states in Aharonov-Bohm graphene quantum rings](#)

J. Appl. Phys. **114**, 214314 (2013); 10.1063/1.4842715

[Graphene nanodots with intrinsically magnetic protrusions](#)

J. Chem. Phys. **136**, 064706 (2012); 10.1063/1.3684900


[Graphene magnet realized by hydrogenated graphene nanopore arrays](#)

Appl. Phys. Lett. **99**, 183111 (2011); 10.1063/1.3653286

[Magnetism and bonding in graphene nanodots with H modified interior, edge, and apex](#)


J. Chem. Phys. **135**, 084707 (2011); 10.1063/1.3624526

Agilent's Electronic Measurement Group is becoming **Keysight Technologies**.



Engineering Education & Research Resources DVD 2014

Agilent is the key to your test and measurement needs **Order yours**



High-efficiency graphene nanomesh magnets realized by controlling mono-hydrogenation of pore edges

T. Kato,¹ T. Nakamura,² J. Kamijyo,¹ T. Kobayashi,¹ Y. Yagi,¹ and J. Haruyama^{1,a)}

¹Faculty of Science and Engineering, Aoyama Gakuin University, 5-10-1 Fuchinobe, Sagamihara, Kanagawa 252-5258, Japan

²Institute for Solid State Physics, The University of Tokyo, 5-1-5 Kashiwanoha, Kashiwa, Chiba 277-8581, Japan

(Received 2 April 2014; accepted 15 June 2014; published online 25 June 2014)

We demonstrate a drastic improvement in the efficiency of rare-element-free graphene nanomesh (GNM) magnets with saturation magnetization values as large as $\sim 10^{-4}$ emu/mm², which are 10–100 times greater than those in previous GNM magnets hydrogenated by only annealing under a hydrogen molecule (H₂) atmosphere, even at room temperature. This improvement is realized by a significant increase in the area of the mono-H-terminated pore edges by using hydrogen silsesquioxane resist treatment with electron beam irradiation, which can produce mono-H by detaching H-silicon (Si) bonds. This result must open the door for industrial applications of graphene magnets to rare-element-free magnetic and spintronic systems. © 2014 AIP Publishing LLC. [<http://dx.doi.org/10.1063/1.4885390>]

The use of magnetic rare-(earth)-metals for magnets and other magnetic systems is facing serious problems owing to the environmental contamination and limited material-resources, although a variety of ferromagnetic metals (e.g., neodymium (Nd), iron, cobalt, chromium) and also ferromagnetic semiconductors (e.g., (In, Mn)As) are used. Hence, it is crucial to develop rare-magnetic-element-free magnets.

On the other hand, it is theoretically predicted that graphene edges with zigzag-type atomic structures provide flat energy bands and subsequently produce an extremely high density of localized electrons (i.e., edge states).^{1,2} Edge states cause strong spin interactions, which leads to the emergence of spontaneously polarized spins states and flat-band ferromagnetism. More importantly, these phenomena occur despite the absence of rare magnetic elements, based on just carbon atoms with sp^2 hybrid orbitals. Graphene nanoribbons (GNRs; one-dimensional structures of graphene with two edges along the longitudinal directions on both sides; Fig. 1)^{3–5} can also cause spontaneous spin polarizations, which are highly sensitive to the kinds of impurities terminating the edges and, consequently, the spin interaction between the two edges, so as to maximize the exchange energy gain (similar to Hund's rule in atoms).

Previously, we developed graphene nanomesh (GNM) magnets,^{6,7} which consist of a honeycomb-like array of hexagonal nanopores with hydrogenated zigzag-type atomic structures on the pore edges and correspond to a large ensemble of hydrogen (H)-terminated zigzag-edged GNRs in the inter-pore regions (Fig. 1(a)). The pore edges allowed the emergence of spontaneously polarized electron spins and subsequently flat-band ferromagnetism due to the edge states, despite the absence of magnetic rare-elements. The formation of a zigzag-type atomic structure of pore edges caused by edge reconstruction was confirmed by observation

of a significant reduction in the G/D peak ratios (I_G/I_D) by critical-temperature annealing in the Raman spectrum and comparison with other experiments (e.g., extremely low I_G/I_D peak ratios in the intentionally fabricated zigzag-edge hexagonal pores⁸ and in the zigzag-edged graphene flakes,⁹ atomic reconstruction of edges to the zigzag structure by STM-Joule heating¹⁰ and high-energy electron beam irradiation¹¹). Moreover, observation of ferromagnetism induced by decreasing the inter-pore distance (i.e., width of the inter-pore GNR regions)⁷ and the high density of polarized spins

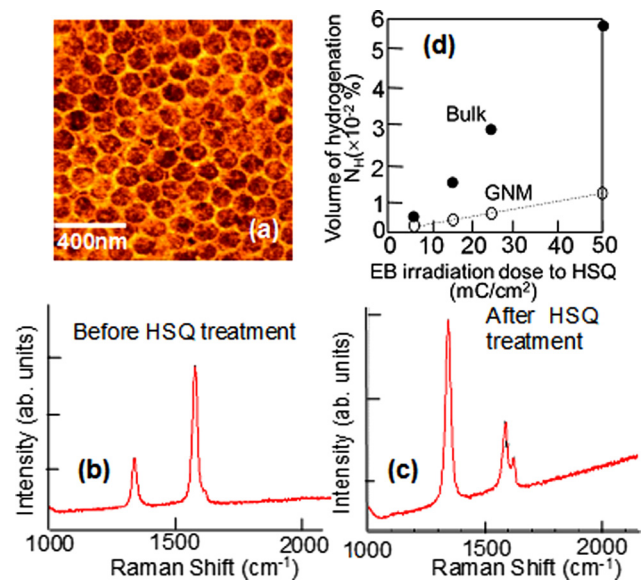


FIG. 1. (a) Atomic force microscope image of the GNM fabricated by a non-lithographic method, which used a nano-porous alumina template as an etching mask of bulk CVD-grown graphene, realizing low contamination and defects of the pore edges. Mean diameter and inter-pore distance are ~ 90 and ~ 20 nm, respectively. Examples of the Raman spectrum (b) before and (c) after the HSQ resist treatment (EB dose of 50 mC/cm²) of GNMs. (d) The relationship of the hydrogenation volume vs. EB irradiation dose in GNMs (open symbols) and bulk CVD-graphenes (filled symbols). Dotted linear line is a guide for the eyes.

^{a)}Author to whom correspondence should be addressed. Electronic mail: J-haru@ee.aoyama.ac.jp

at the pore edges by magnetic force microscopy in the ferromagnetic GNM (FGNM)⁷ suggested that the observed ferromagnetism originated from the presence of polarized spins existing at the pore edges. Two different theoretical analyses (i.e., GNR theory and Lieb's theorem) for the observed magnetization values ($\sim 0.3 \mu_B/\text{edge}$ dangling bond) also suggested that the mono-hydrogenated zigzag pore edges were the cause for ferromagnetism. Furthermore, edge states in FGNMs have been reconfirmed by observation using ionic-liquid gates.¹² Novel tunneling magnetoresistance devices have also been developed in FGNM/SiO₂/cobalt tunneling junctions, based on the specified spin alignment of pore edges.¹³

However, the magnitude of ferromagnetism in FGNMs was still small (e.g., $\sim 10^{-6}$ emu/mm²) owing to the following two problems; i.e., the insufficient density (or area) of (1) zigzag pore edges, which are only produced by the critical-temperature annealing for the reconstruction of edge atomic structures, and (2) the mono-H-termination of zigzag pore edges only performed using critical-temperature annealing under H₂ atmosphere. To improve the former problem, alignment of the honeycomb-like array of the hexagonal pore to the honeycomb carbon lattice of graphene is highly expected. In addition, thermo-carbon etching of the pore edges after non-intentional formations of the pore with the arm-chair edge will be effective. In contrast, to resolve the latter problem, it is indispensable that an effective mono-H-termination method is developed because di-H-termination (H₂-termination) of zigzag-type pore edges cannot lead to a large ferromagnetism.⁶ In the present study, we report a significant increase in the ferromagnetism amplitude (10–100 times) realized by the control of mono-H-termination using hydrogen silsesquioxane (HSQ) resist treatment with electron beam (EB) irradiation.

Recently, introduction of the colossal spin-orbit interaction (SOI; with a spin relaxation time of ~ 90 ps and a spin-orbit (SO) strength of ~ 2.5 meV in 0.01%-hydrogenated graphene), which originates from the formation of the *sp*³ carbon bonds by hydrogenation and broken symmetry along the z-axis (out-of-plane) direction (i.e., Rashba-type SO scattering), and the spin-Hall effect (SHE) were reported in graphenes precisely hydrogenated using a HSQ resist (HSiO_{3/2})_n with EB irradiation.^{14–16,18} We have also reconfirmed SOI and SHE under a strong interaction with the spin phase interference phenomena.¹⁷

In the present study, HSQ resist treatment was performed on GNM fabricated using our previous method.^{6,7} Atomic force microscope image of the GNM is shown in Fig. 1(a). The GNM was fabricated by a non-lithographic method using nano-porous alumina templates (with ~ 1.5 mm² area) as the etching mask for chemical vapor deposition (CVD)-grown graphenes on SiO₂, which realized low defects and low contaminations of the pore edges. Right after the critical temperature annealing (at 800 °C), which is required for the formation of the zigzag pore edges by atomic reconstruction, HSQ resist treatment was performed on this GNM.

The mono-H-termination of pore edges can be basically realized using EB irradiation to the HSQ resist. The HSQ resist (HSiO_{3/2})_n consists of H, Si, and O atoms. The atomic bonds related to H (i.e., H-Si and H-O bonds) are easily

detached by EB irradiation, and atomic H species can be produced from the HSQ resist because the binding energy of H-Si is ~ 3 eV, whereas EB irradiation energy is larger than 1 KeV even at the smallest case.¹⁸ Here, [EB irradiation dose] is given by [irradiation energy] \times [irradiation time]. In our case, the irradiation energy was fixed around 10 keV. Thus, it is assumed that the excess dose depending on irradiation time can contribute to formation of C-H bonds with a binding energy of ~ 2.2 eV through mono-H termination of the dangling bonds at the zigzag pore edges by the detached H-atoms in GNM as well as the mono-hydrogenation of the narrow interpore bulk GNR regions. On the other hand, in our previous H-termination method of the pore edges, we employed high-temperature annealing only under H₂ atmosphere, leading to H₂-termination on most parts of the pore edges and also just small parts of occasional mono-H-termination. Because only mono-H-termination of zigzag edges can produce a large flat-band ferromagnetism,⁶ these two terminations cannot result in a large ferromagnetism, and thus, the saturation magnetization values in our previous GNM were small.

Figures 1(b) and 1(c) show examples of Raman spectra of the GNM before and after HSQ resist treatment, respectively. Even before HSQ treatment, I_D is slightly high due to presence of the pores⁷ compared to those in bulk graphenes, whereas I_D value significantly increases due to the mono-H-termination of the zigzag pore edges as well as that in the interpore bulk GNR regions after HSQ treatment as reported in Ref. 14. The volume of hydrogenation (i.e., area of hydrogenation) in bulk graphenes was estimated from the I_G/I_D ratios in the Raman spectra following the procedure described in Ref. 14. Excluding contribution of the pore edges and damages by EB irradiation to I_D, the empty round symbols of Fig. 1(d) show the hydrogenation volume estimated from Raman spectra vs. EB dose in GNM. It implies a linear relationship. Moreover, because the pore diameter is ~ 80 nm and interpore distance is ~ 20 nm, $\sim 80\%$ of a GNM are pores. Hence, hydrogenation volume of a GNM drastically decreases at an individual dose compared with those in bulk graphenes shown by filled symbols. The decrease from bulk graphenes to GNM is approximately 20% in Fig. 1(d). This suggests the presence of not di-H-termination (H₂-termination) but mono-H-termination of the pore edge dangling bonds because individual C-atoms in bulk graphenes are mono-hydrogenated and the mono-H-termination of pore edge dangling bonds in GNM is similar to it. If the pore edges are H₂-terminated, the decrease in the hydrogenation volume should be greatly suppressed.

Examples of the GNM magnetization curves for the two different EB irradiation doses in Fig. 1(d) are shown in Figs. 2(a) and 2(b) at T = 2 and 300 K, respectively. We find that reducing the irradiation dose by half exactly decreases the saturation magnetization by half. Measurement results of the saturation magnetization values as a function of the hydrogenation volume of Fig. 1(d) are shown in Fig. 2(c), including the results shown in Figs. 2(a) and 2(b). A linear relationship is confirmed. Moreover, we obtained 10–100 times increase in the saturation magnetization for the present GNM compared to those in the previous GNM, which were H₂-terminated only by high-temperature annealing

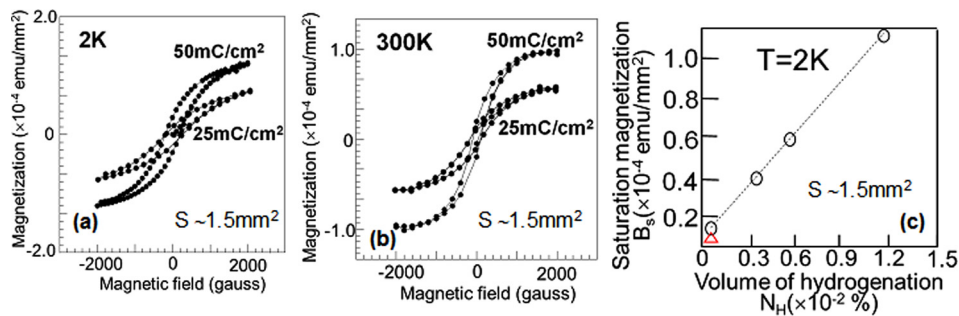


FIG. 2. Magnetization curves of HSQ-GNMs for two different EB irradiation doses at (a) 2 and (b) 300 K. (c) The relationship between the saturation magnetization in HSQ-GNMs including the results of (a) and the hydrogenation volume shown in Fig. 1(d). Dotted linear line is a guide for the eyes. The red triangular symbol shows an example of the maximum magnetization value of a GNM hydrogenated by our previous method using H₂ annealing.

under an H₂ atmosphere. An example of the maximum magnetization value of the previous GNMs was shown by a red triangle symbol in Fig. 2(c). The magnetization value corresponds to hydrogenation volumes less than $0.1 \times 10^{-2}\%$ in the present GNMs. It suggests much smaller mono-H-termination of the pore edges in the previous GNMs.

These results imply that the edge dangling bonds have certainly been mono-H-terminated, which leads to the appearance of the flat-band ferromagnetism, because neither the hydrogenation of defects (impurities), which exist randomly on GNMs, nor the H₂-termination of the pore edges can lead to the linear relationship shown in Fig. 2(c). Since the edge dangling bonds of the zigzag nanopores exist uniformly in GNMs, an increase in the volume (area) of the mono-H-termination can yield the linearity shown in Fig. 2(c). In the present GNMs, the interpore GNR width is as small as ~20 nm, whereas the pore diameter is ~80 nm with ~1000 edge dangling bonds. Thus, hydrogenation was mostly concentrated on the H-termination of the pore edge dangling bonds, and it leads to evident changes in magnetism with the linear relationship.

To reconfirm the relationship between the mono-H-terminated area and magnetization, we measured the GNM magnetizations with various sample areas, which were hydrogenated under identical EB irradiation doses (50 mC/cm²). The results are shown in Fig. 3. It is found that saturation magnetization values linearly depend on the area of GNMs. This result strongly supports that the ferromagnetism originates from the mono-H-termination per pore-edge dangling bond and that the increase in the mono-H-terminated area,

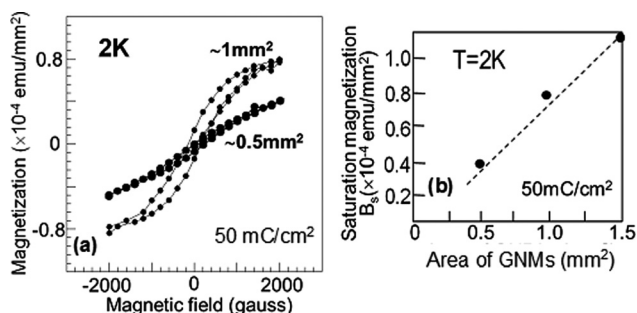


FIG. 3. (a) Magnetization curves of HSQ-GNMs with different sample areas, which were hydrogenated under the same EB irradiation dose (50 mC/cm²). (b) The relationship between the saturation magnetization and area of GNMs, which includes the area of the nanopores. Dotted linear line is a guide for the eyes.

which linearly depends on EB irradiation dose, yields the linearity shown in Fig. 2(c).

In conclusion, we demonstrated a drastic improvement of the flat-band ferromagnetism of the GNM-magnets up to an order of $\sim 10^{-4}$ emu/mm², which is 10–100 times greater than those in our previous GNM magnets hydrogenated only by annealing under H₂ atmosphere. The improvement was realized by the increase in the mono-H-terminated pore area by controlling the pore edge hydrogenation using an HSQ resist treatment with EB irradiation. The magnetic properties (e.g., coercivity $H_c \sim 0.7 \times 10^{-4}$ emu/mm² and residual magnetization $B_r \sim 200$ G at 2 K in a GNM with EB dose of 50 mC/cm², as well as, the saturation magnetization $\sim 1.2 \times 10^{-4}$ emu/mm²) of the present HSQ-GNMs should be still improved further compared with those in recent magnets (e.g., $H_c \sim 2$ T and saturation magnetization ~ 2 T in Nd₂Fe₁₄B magnets). However, adding this new function to the original properties of graphenes (e.g., highly conductive, transparent, flexible, and ultra-light), this result must open the door to rare-(earth)-element-free magnetic and spintronic systems, which can resolve current problems for the environmental contamination and limited material-resources.

The authors thank S. Katsumoto, M. Yamamoto, S. Tarucha, H. Hibino, K. Sugawara, T. Ando, T. Enoki, J. Akimitsu, T. Muranaka, Y. Yagi, A. H. Castro Neto, B. Özyilmazet, S. Roche, and M. S. Dresselhaus for their technical support, fruitful discussions, and continuous encouragement. This work at Aoyama Gakuin was partly supported by a Grant-in-aid for Scientific Research (Basic Research A: 24241046) in MEXT and AFOSR grant.

¹K. Nakada, M. Fujita, G. Dresselhaus, and M. S. Dresselhaus, *Phys. Rev. B* **54**, 17954 (1996).

²K. Kusakabe and M. Maruyama, *Phys. Rev. B* **67**, 092406 (2003).

³T. Shimizu, J. Haruyama, D. C. Marcano, D. V. Kosynkin, J. M. Tour, K. Hirose, and K. Suenaga, *Nat. Nanotechnol.* **6**, 45 (2011).

⁴S. Kamikawa, T. Shimizu, Y. Yagi, and J. Haruyama, *Nanomater. Nanotechnol.* **4**(12), 1 (2014).

⁵D. Soriano, N. Leconte, P. Ordejón, J.-C. Charlier, J.-J. Palacios, and S. Roche, *Phys. Rev. Lett.* **107**, 016602 (2011).

⁶K. Tada, J. Haruyama, H. Yang, and M. Chshiev, *Physica Status Solidi B* **249**, 2491 (2012).

⁷T. Shimizu, J. Nakamura, K. Tada, Y. Yagi, J. Haruyama et al., *Appl. Phys. Lett.* **100**, 023104 (2012).

⁸B. Krauss, P. Incze, V. Skakalova, L. P. Biro, K. von Klitzing, and J. Smet, *Nano Lett.* **10**, 4544 (2010).

⁹Y. You, Z. Ni, T. Yu, and Z. Shen, *Appl. Phys. Lett.* **93**, 163112 (2008).

- ¹⁰X. Jia, M. Hofmann, V. Meunier, B. G. Sumpter, J. Cam-pos-Delgado, J. M. Romo-Herrera, H. Son, Y. Hsieh, A. Reina, J. Kong, and M. S. Dresselhaus, *Science* **323**, 1701 (2009).
- ¹¹Ç. Ö. Girit, J. C. Meyer, R. Erni, M. D. Rossell, C. Kisielowski, L. Yang, C. Park, M. F. Crommie, M. L. Cohen, and S. G. Louie, *Science* **323**, 1705 (2009).
- ¹²T. Hashimoto, S. Kamikawa, Y. Yagi, and J. Haruyama, *Mater. Sci. Appl.* **5**(1), 1 (2014).
- ¹³S. Kamikawa, J. Haruyama, D. Soriano, and S. Roche, "Rare-metal free tunneling magnetoresistance phenomenon arising from edge spins of magnetic graphene nanopore arrays," *Nat. Nanotechnol.* (unpublished), URL: <http://www.ee.aoyama.ac.jp/haru-lab/>.
- ¹⁴J. Balakrishnan, G. K. W. Koon, M. Jaiswal, A. H. Castro Neto, and B. Özyilmaz, *Nat. Phys.* **9**, 284 (2013).
- ¹⁵B. Özyilmaz, P. Jarillo-Herrero, D. Efetov, and P. Kim, *Appl. Phys. Lett.* **91**, 192107 (2007).
- ¹⁶S. W. Nam, M. J. Rooks, J. K. W. Yang, K. K. Berggren, H. M. Kim, M. H. Lee, and K. B. Kim, *J. Vac. Sci. Technol. B* **27**(6), 2635 (2009).
- ¹⁷J. Kamijyo, T. Nakamura, S. Katsumoto, and J. Haruyama, "Spin phase interference correlated to spin-orbit interaction in hydrogenated graphenes," *Nat. Commun.* (unpublished), URL: <http://www.ee.aoyama.ac.jp/haru-lab/>.
- ¹⁸D. L. Olynick, B. Cord, A. Schipotinin, D. F. Ogletree, and P. J. Schuck, *J. Vac. Sci. Technol. B* **28**, 581 (2010).